

Improving Prediction of Oil Well Performance

Carter Shaver, SPE Marietta College

INTRODUCTION

The procedure for predicting an inflow performance (IPR) curve for an oil well involves first measuring a well's current average reservoir pressure and then flowing the well at a constant rate until the bottom-hole pressure stabilizes. Under ideal circumstances, the well's flow efficiency is also determined.

This data is used in conjunction with dimensionless IPR curves developed by Vogel² for flow efficiencies equal to 1 or by Standing³ for flow efficiencies not equal to 1 to predict the current IPR curve for the well.

Future IPR curves can be determined using a technique developed by Echmeir⁵ to solve for $q_{o\max}$ at future conditions using equation (1):

$$q_{o\max i} / q_{o\max f} = (\bar{P}_{r i} / \bar{P}_{r f})^3 \dots\dots\dots(1)$$

Knowing the value of $q_{o\max f}$ at the future average reservoir pressure, one can generate a new IPR curve using Vogel's or Standing's procedures.

The use of Vogel's Method for predicting IPR curves is a widely assumed standard in industry today. This research will reveal how inaccuracies may be introduced into this procedure depending on the points used to determine the Vogel IPR curve. It will also examine an alternative method to predict IPR curves that yields more reliable results.

OBJECTIVE

This paper will examine the methods used to predict the current and future deliverability of oil wells, analyze the qualitative and quantitative results of the procedures, and conclude on the best method to establish an accurate representation of the future deliverability of an oil well.

This research involves evaluating a new methodology for predicting future IPR curves for oil wells based on a method developed for gas wells. For this procedure, known flowing bottom-hole pressures and oil flow rates are needed. The production data employed is from an IPR curve experimentally obtained in the

field for an oil well in the Carry City field, Oklahoma as reported in *Well Performance* by Michael Golan and Curtis H. Whitson¹. A future IPR curve was not reported and had to be developed using a method referred to as the United States Bureau of Mines (USBM) Four-Point Test Method⁴.

The main purpose of this research was to determine the best method to predict future IPR curves for oil wells by evaluating which single flowing point used in Vogel's IPR equation resulted in the most accurate values of current and future $q_{o,max}$. In addition, it was desired to know which 2-points used in Chase's method for determining current and future IPR curves yielded the most accurate representation of the actual current and future $q_{o,max}$. The research also examines the discrepancies that can result from using Vogel's IPR to predict oil well deliverability.

METHOD

Golan and Whitson presented a complete current IPR curve obtained in the field by measuring stabilized bottom-hole pressures as a function of declining flow rate. This data can be seen in Table 1 and Figure 1.

Point	P_{wf}/P_r	P_{wf} (psia)	Q_o (stb/d)
0	0.00	0	2500
1	0.10	166	2435
2	0.11	183	2460
3	0.22	351	2352
4	0.33	534	2260
5	0.49	787	1965
6	0.54	867	1895
7	0.62	996	1765
8	0.67	1066	1625
9	0.75	1194	1470
10	0.79	1267	1260
11	0.84	1342	1045
12	0.92	1470	720
13	0.92	1476	610
14	0.94	1497	565
15	0.97	1558	235
16	1.00	1600	0

Table 1—Production Data

In turn, they plotted the measured flow rates versus average reservoir pressure squared minus the corresponding flowing bottom-hole pressure squared on a log-log plot to obtain a straight line. Figure 2 displays the plot and the power-type trend line equation. This is similar to that obtained from a conventional backpressure test on a gas well.

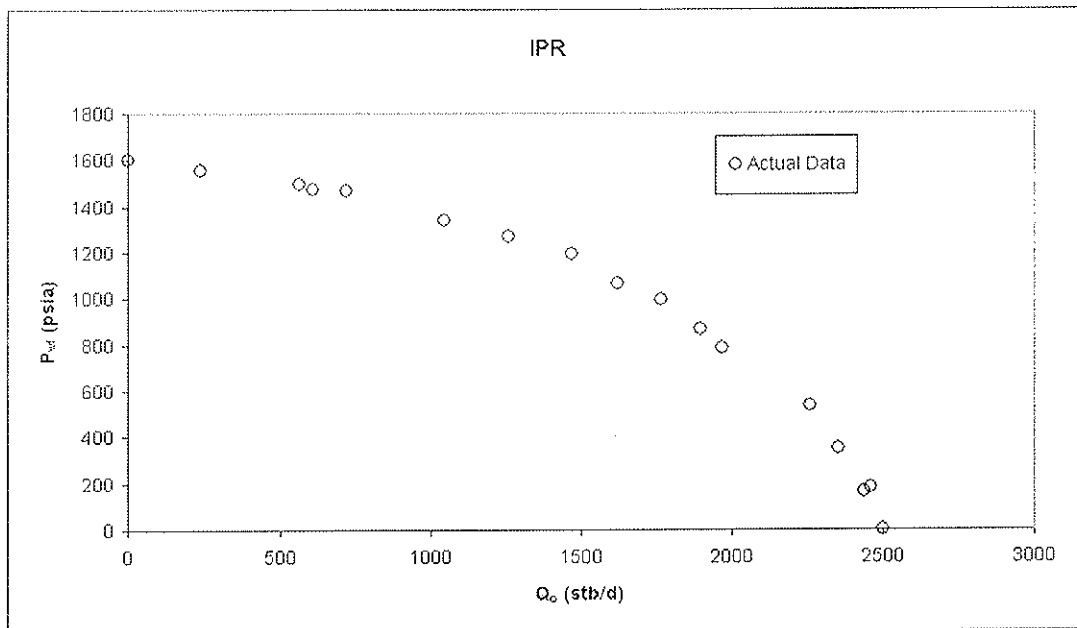


Fig. 1—Actual IPR (from Golan and Whitson)

The equation describing the line is known as the stabilized deliverability curve (SDC) equation and is:

$$Q = C (\bar{P}_r^2 - P_{wf}^2)^n \dots\dots\dots(2)$$

Where,

$$n = 1/\text{slope of the line} \dots\dots\dots(3)$$

$$C = Q/(\bar{P}_r^2 - P_{wf}^2)^n \dots\dots\dots(4)$$

Both Q and ΔP^2 in equation 4 must be taken from a point on the trend line. From this plot and evaluation, the stabilized deliverability equation for the production data in table 1 was ascertained to be:

$$Q = 0.0805 (\bar{P}_r^2 - P_{wf}^2)^{0.700} \dots\dots\dots(5)$$

Equation 5 can be used to predict both the present and future inflow performance of the well in question. This is done by assuming a value for \bar{P}_r , choosing values for P_{wf} , and solving for flow rates. This procedure encompassing the log-log plot and subsequent equations will be used repeatedly and will be referred to as the ΔP^2 method.

The ΔP^2 -generated IPR was then compared to the actual production data IPR as shown in Appendix A confirming the ΔP^2 method was consistent with the actual current data and therefore can be used to predict future IPR curves.

The next scenario used \bar{P}_r , one flow test point and Vogel's method to generate an IPR. In order to utilize Vogel's equation, one flowing point must be known. The point used in this method was varied to show the impact of rate selection on the shape and position of the resulting IPR curves. The specific points used are labeled in Table 1 as point 13, 10, 7, 5, and 3. The resulting IPR curves from Vogel's method are compared to those generated using the ΔP^2 method using two flow points. Reference Appendix C for flow rate values.

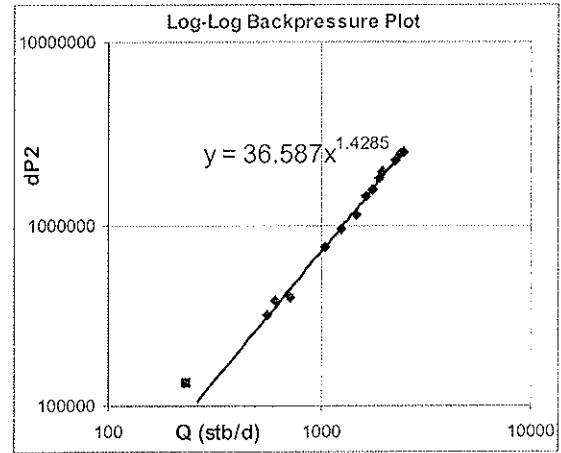


Fig. 2—Log-Log Backpressure Plot

In the ΔP^2 method using two flow points, point 15 is the “anchor point” and is used in combination with points 13, 10, 7, 5, and 3, as labeled in Table 1. Accordingly, point 15 and one flow point are plotted on log-log paper to determine the SDC equation that is used to generate a ΔP^2 IPR curve.

Figure 3 demonstrates the procedure for flow point 13. This procedure was repeated for all the points mentioned and an SDC equation was developed for each corresponding point. Appendix E displays plots for points 13, 10, 7, 5, and 3 of the Vogel IPR one-point plot, ΔP^2 plot, and the actual production data plot. Reference Appendix D for flow rate values.

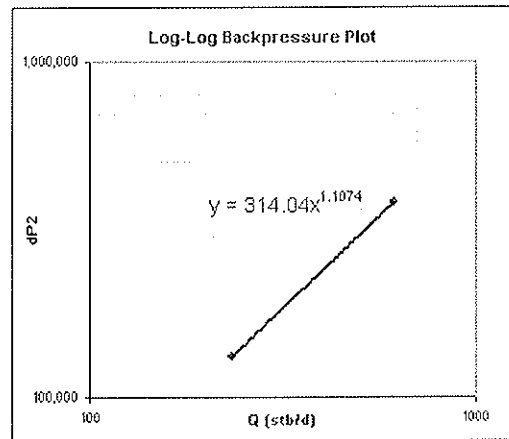


Fig. 3—Point 13 Log-Log Backpressure Plot

The final set of plots constructed show the future IPR curves generated for future conditions. First, future IPR curve data were generated by using equation 5 and a future \bar{P}_r of 1066 psia.

Second, Echmeir's method for determining a future $q_{o\max}$ in conjunction with Vogel's IPR for each point (13, 10, 7, 5, and 3) was constructed. A future $q_{o\max}$ was found from the original $q_{o\max}$ and this future $q_{o\max}$ was used in Vogel's equation to generate new, future flow rates.

Third, a future IPR curve in conjunction with the ΔP^2 method was developed using the future \bar{P}_r of 1066 psia in equation 2 for each flow point (13, 10, 7, 5, and 3).

For each of these points, both the future Vogel IPR curve using Echmeir's future $q_{o\max}$ and the ΔP^2 method future IPR were plotted versus the data generated using equation 5. These graphs can be seen in Appendix F.

DISCUSSION OF RESULTS

Through comparison of the IPR curves for the actual production data shown in Figure 1 with the IPRs generated using the single-point Vogel method and the ΔP^2 method it was found that Vogel's method using a single point from the original production data consistently over-predicted the actual $q_{o\max}$. This can be seen in the plot in Appendix G.

IPR curves generated using Vogel's method are most accurate when a value of Q is obtained at a value of P_{wf} equal to $0.1 \bar{P}_r$. For example, using point 3 to create a future IPR curve resulted in only a 3% error between the predicted Vogel $q_{o\max}$ and the actual $q_{o\max}$. Using point 13, however, resulted in an 81% percent difference in $q_{o\max}$ values. The shape of the IPR curve found using Vogel's method also proved to be inaccurate.

The graph in Appendix H displays the ΔP^2 method versus the actual production data. This graph shows the ΔP^2 method to accurately predict the $q_{o\max}$ for a wider range of P_{wf}/\bar{P}_r

values. Quantitatively, there is less than 17% $q_{o\max}$ error when $P_{wf} < 0.9 \bar{P}_r$. Additionally, the shape of the actual production data is best represented by the generated ΔP^2 method curve.

Appendix F contains the plotted future IPR curve scenarios for the actual generated future production data, the future Vogel IPR curve, and the future ΔP^2 method curve. Converse to the current Vogel data, these plots showed Vogel (Echmeir $q_{o\max}$) to under-predict the actual future $q_{o\max}$. When P_{wf}/\bar{P}_r approached 1 (Point 13) introduces a 4% error from the actual future $q_{o\max}$ compared to P_{wf}/\bar{P}_r approached 0.8 (Point 10), which introduces a 21% error from the actual future $q_{o\max}$. The error significantly increases as P_{wf}/\bar{P}_r approaches 0.1. Table 2 shows the percentage of error between the actual $q_{o\max}$ and the future Vogel and future ΔP^2 $q_{o\max}$.

	P_{wf}/\bar{P}_r	Future Vogel % Error	Future ΔP^2 % Error
Point 13	0.92	4%	17%
Point 10	0.79	21%	5%
Point 7	0.62	34%	3%
Point 5	0.49	41%	8%
Point 3	0.22	46%	8%

Table 2— $q_{o\max}$ Deviation

The future ΔP^2 IPR curve most accurately predicts the shape and $q_{o\max}$ for values of $0.2 < P_{wf}/\bar{P}_r < 0.8$. For points of $P_{wf}/\bar{P}_r < 0.8$, the error increases from 5% up to 17% (Point 10 and 13 respectively). For points in the acceptable range (points 10, 7, 5, 3) the average error is 6%. The future flow rate data for each individual point (Vogel and ΔP^2) is presented in the table in Appendix D.

CONCLUSION

The best method for determining future IPR curves is to utilize the ΔP^2 method for two flow rates flowed to a stabilized P_{wf} . Both P_{wf} values

should be greater than $0.8 \bar{P}_r$. This produces the most accurate current and future IPR curves with an insignificant q_{omax} error.

Note that only one set of data could be found in the literature in which a complete IPR curve was actually constructed. Further investigation should be conducted on more data sets to confirm these findings.

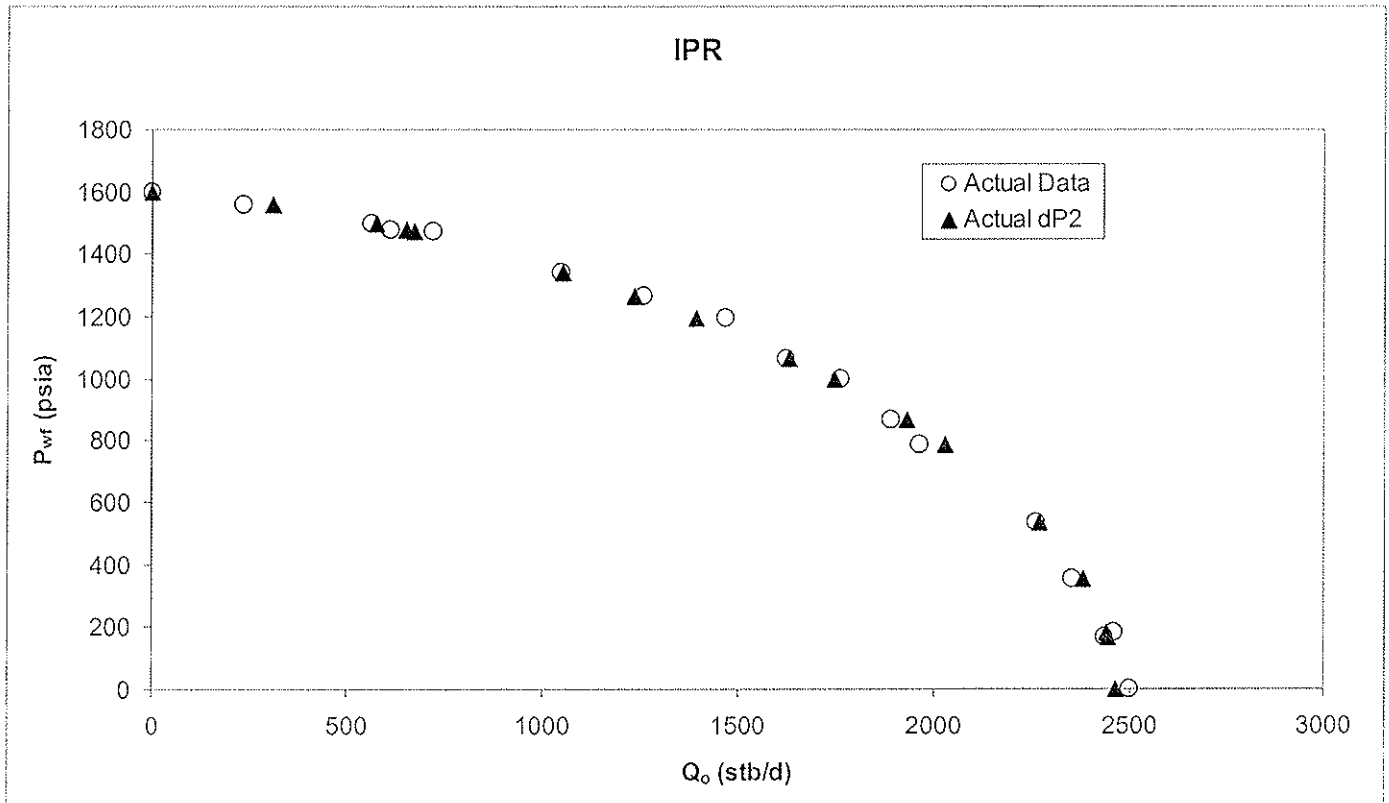
ACKNOWLEDGMENTS

The development of the method presented was influenced by the concepts of Dr. Bob Chase and I would like to sincerely thank him for his insight and review on this research.

REFERENCES

1. Golan, M. and Whitson, C.H.: *Well Performance*. Prentice Hall, Englewood Cliffs, NJ (1986).
2. Vogel, J.V.: "Inflow Performance Relationships For Solution-Gas Drive Wells," *JPT*. (Jan. 1968) 83-92; *Trans.*, AIME, 243.
3. Standing, M. B.: "Concerning the Calculations of Inflow Performance of Wells Producing From Solution-Gas Drive Reservoirs," *JPT*. (1947) 1141-1142.
4. Rawlings, E.L. and Schellhardt, M.A.: *Back-Pressure Data on Natural Gas Wells and Their Application to Production Practices*, U.S. Bureau of Mines Monograph 7 (1936).
5. Kermit, B.E.: *The Technology of Artificial Lift*. Vol. 4. "Production Optimization of Oil and Gas Wells By Nodal Systems Analysis," 1984.

Appendix A—Actual IPR Curve and ΔP^2 -Generated IPR Curve



Appendix B—Current Vogel Flow Rate Values

Point	F_{wf}/P_i	P_{wf} (psia)	Q_o (stb/d)	Pnt 13		Pnt 10		Pnt 7		Pnt 5		Pnt 3	
				Vogel Q_o (stb/d)	R^2	Vogel Q_o (stb/d)	R^2	Vogel Q_o (stb/d)	R^2	Vogel Q_o (stb/d)	R^2	Vogel Q_o (stb/d)	R^2
0	0.00	0	2500	4529	0.81	3706	3121	2775	2563	-0.03			
1	0.10	166	2435	4396	0.81	3597	3030	2694	2488	-0.02			
2	0.11	183	2460	4378	0.78	3583	3017	2683	2478	-0.01			
3	0.22	351	2352	4156	0.77	3401	2864	2547	2352	0.00			
4	0.33	534	2260	3823	0.69	3129	2635	2343	2164	0.04			
5	0.49	787	1965	3207	0.63	2624	2210	1965	1815	0.08			
6	0.54	867	1895	2974	0.57	2434	2050	1822	1683	0.11			
7	0.62	996	1765	2561	0.45	2096	1765	1569	1449	0.18			
8	0.67	1066	1625	2317	0.43	1896	1597	1420	1311	0.19			
9	0.75	1184	1470	1835	0.25	1502	1265	1125	1039	0.29			
10	0.79	1267	1260	1540	0.22	1260	1061	943	871	0.31			
11	0.84	1342	1045	1220	0.17	976	841	748	691	0.34			
12	0.92	1470	720	838	-0.11	492	440	391	361	0.50			
13	0.92	1476	610	610	0.00	469	420	374	345	0.43			
14	0.94	1497	555	510	-0.10	390	351	312	289	0.49			
15	0.97	1558	235	211	-0.10	159	146	130	120	0.49			
16	1.00	1600	0	0	0.39	0	0	0	0	0.21			
					81%		48%		25%		11%		3%

Appendix C—Current ΔP^2 Flow Rate Values

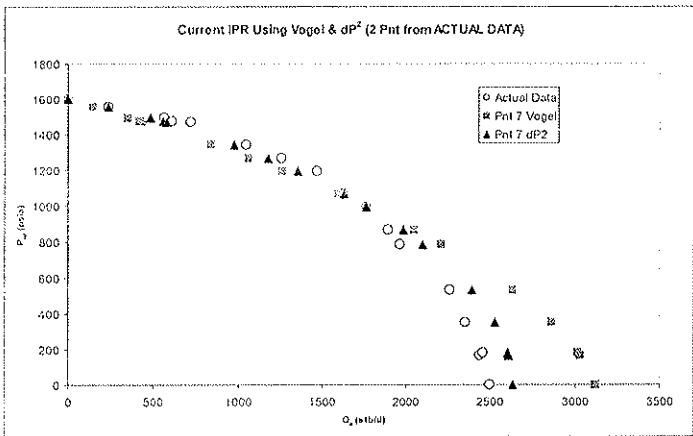
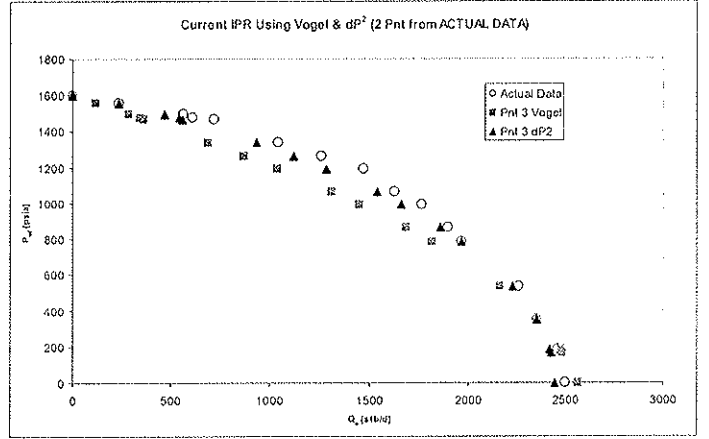
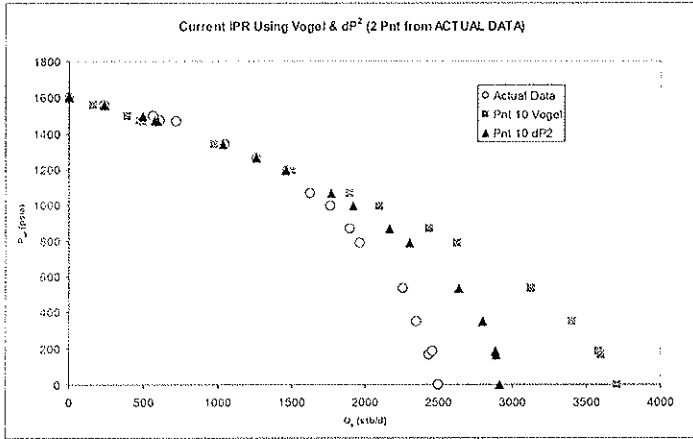
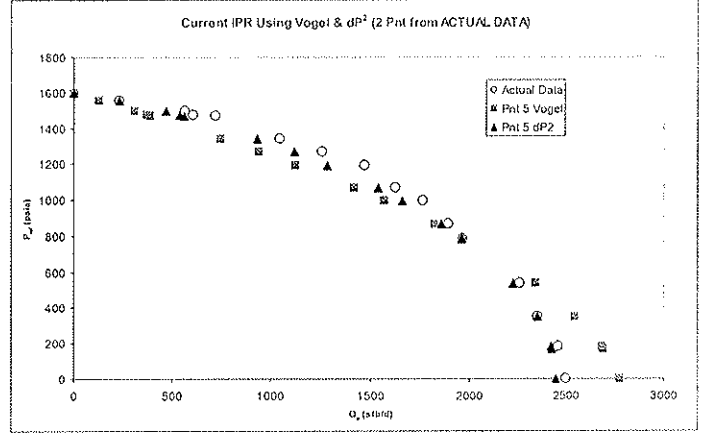
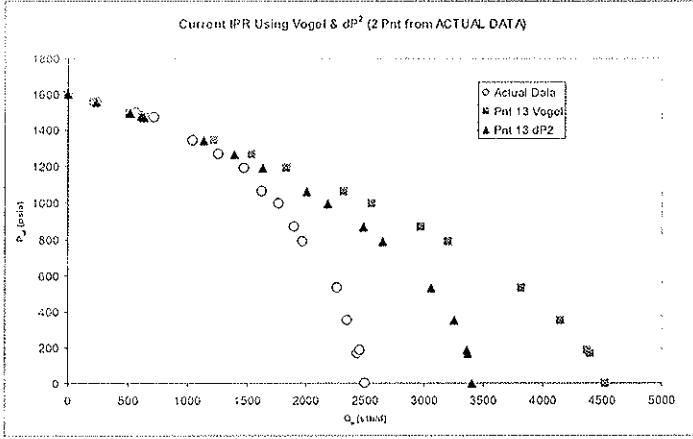
Point	P_{wf}/P_r	P_{wf} (psia)	Q_o (stb/d)	ΔP^2	Actual ΔP^2 Q_o (stb/d)	Pnt 13 ΔP^2		Pnt 10 ΔP^2		Pnt 7 ΔP^2		Pnt 5 ΔP^2		Pnt 3 ΔP^2	
						Q_o (stb/d)	R2	Q_o (stb/d)	R2	Q_o (stb/d)	R2	Q_o (stb/d)	R2	Q_o (stb/d)	R2
0	0.00	0	2500	2560000	2464	3404	-0.38	2916	2633	2446	2446	0.28			
1	0.10	166	2435	2532444	2445	3370	-0.38	2899	2610	2425	2425	0.28			
2	0.11	183	2460	2526511	2441	3363	-0.38	2883	2605	2421	2420	0.28			
3	0.22	351	2352	2436799	2380	3255	-0.37	2796	2529	2352	2352	0.28			
4	0.33	534	2260	2274844	2268	3059	-0.35	2637	2391	2228	2227	0.27			
5	0.49	787	1965	1940631	2030	2650	-0.31	2304	2100	1965	1964	0.26			
6	0.54	867	1895	1808311	1932	2487	-0.29	2169	1983	1858	1857	0.25			
7	0.62	996	1765	1567984	1748	2186	-0.25	1922	1765	1659	1659	0.24			
8	0.67	1066	1625	1423644	1634	2004	-0.23	1770	1631	1537	1537	0.23			
9	0.75	1194	1470	1134364	1394	1632	-0.17	1459	1355	1284	1284	0.21			
10	0.79	1267	1260	954711	1235	1397	-0.13	1260	1177	1121	1120	0.20			
11	0.84	1342	1045	759036	1052	1135	-0.08	1037	976	935	934	0.18			
12	0.92	1470	720	399100	671	835	0.05	800	578	562	562	0.12			
13	0.92	1476	610	381424	650	610	0.06	577	557	542	542	0.11			
14	0.94	1497	565	318991	573	519	0.09	496	481	471	471	0.09			
15	0.97	1558	235	132636	310	235	0.24	235	235	235	235	0.00			
16	1.00	1600	0	0	0	0	-0.18	0	0	0	0	0.21			
						36.1%		16.6%		5.3%		2.2%		2.2%	

Appendix D—Future Flow Data for Vogel and ΔP^2

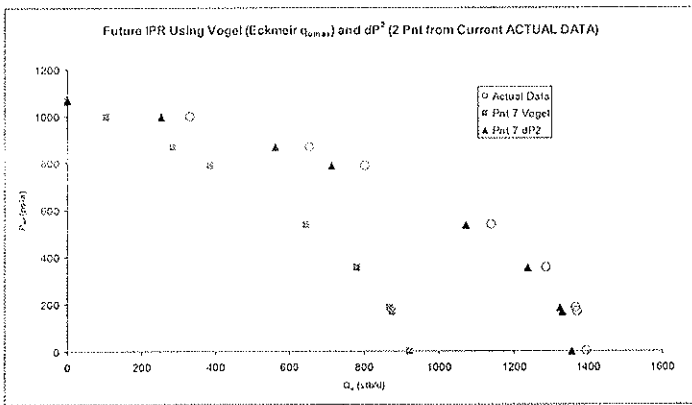
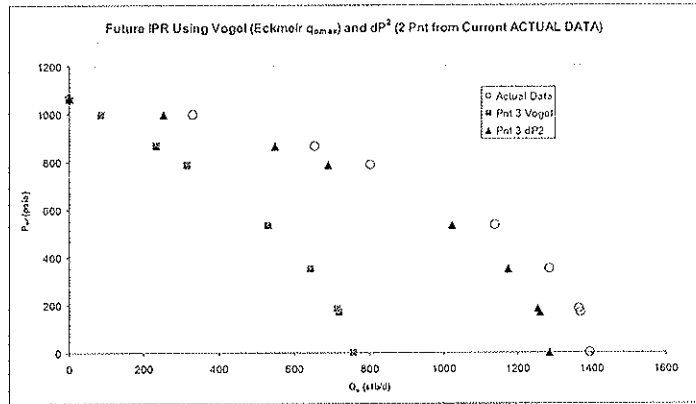
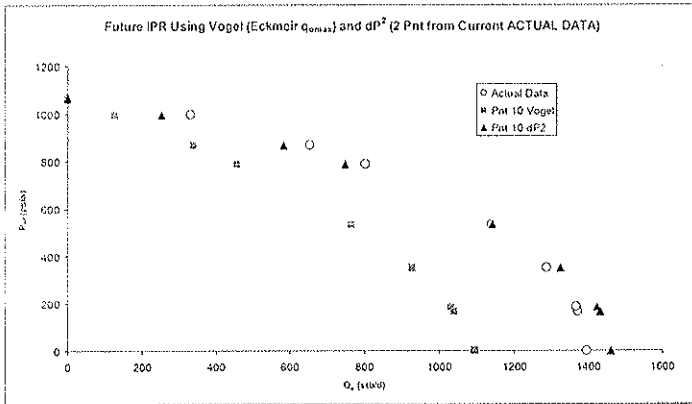
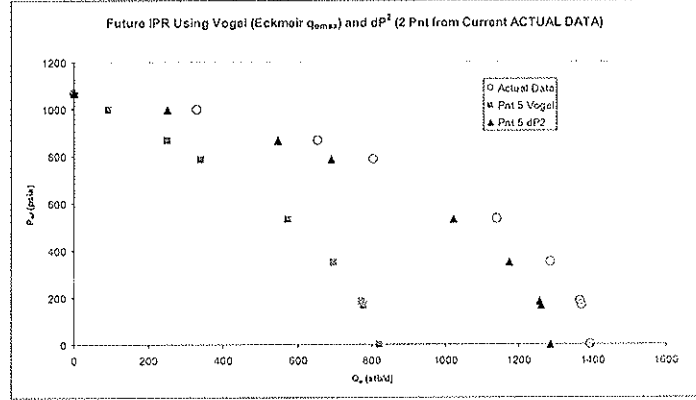
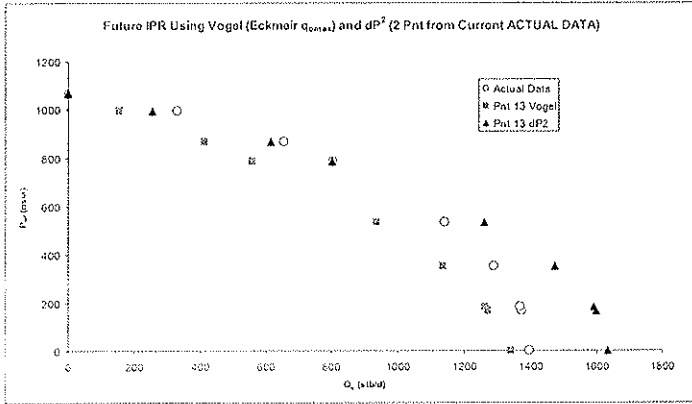
Future @ $P_r = 1066$

Future	Pnt 13		Pnt 10		Pnt 7		Pnt 5		Pnt 3	
	$Q_{o,max} = 1339$		$Q_{o,max} = 1096$		$Q_{o,max} = 923$		$Q_{o,max} = 821$		$Q_{o,max} = 758$	
	$P_r = 1066$		$P_r = 1066$		$P_r = 1066$		$P_r = 1066$		$P_r = 1066$	
Actual ΔP^2 Q_o (stb/d)	Vogel Q_o (stb/d)	ΔP^2 Q_o (stb/d)	Vogel Q_o (stb/d)	ΔP^2 Q_o (stb/d)	Vogel Q_o (stb/d)	ΔP^2 Q_o (stb/d)	Vogel Q_o (stb/d)	ΔP^2 Q_o (stb/d)	Vogel Q_o (stb/d)	ΔP^2 Q_o (stb/d)
1395	1339	1635	1096	1461	923	1357	821	1286	758	1286
1372	1272	1599	1041	1431	876	1330	779	1261	720	1261
1366	1262	1591	1033	1424	870	1324	773	1256	714	1256
1288	1135	1474	929	1325	782	1236	695	1175	642	1174
1140	936	1259	766	1143	645	1072	574	1023	530	1023
804	558	803	456	748	384	713	342	690	316	690
654	413	615	338	581	284	560	253	546	234	546
329	154	254	126	253	106	252	94	251	87	251
0	0	0	0	0	0	0	0	0	0	0
$Q_{o,max}$ % Error From Actual	4%	17%	21%	5%	34%	3%	41%	8%	46%	8%

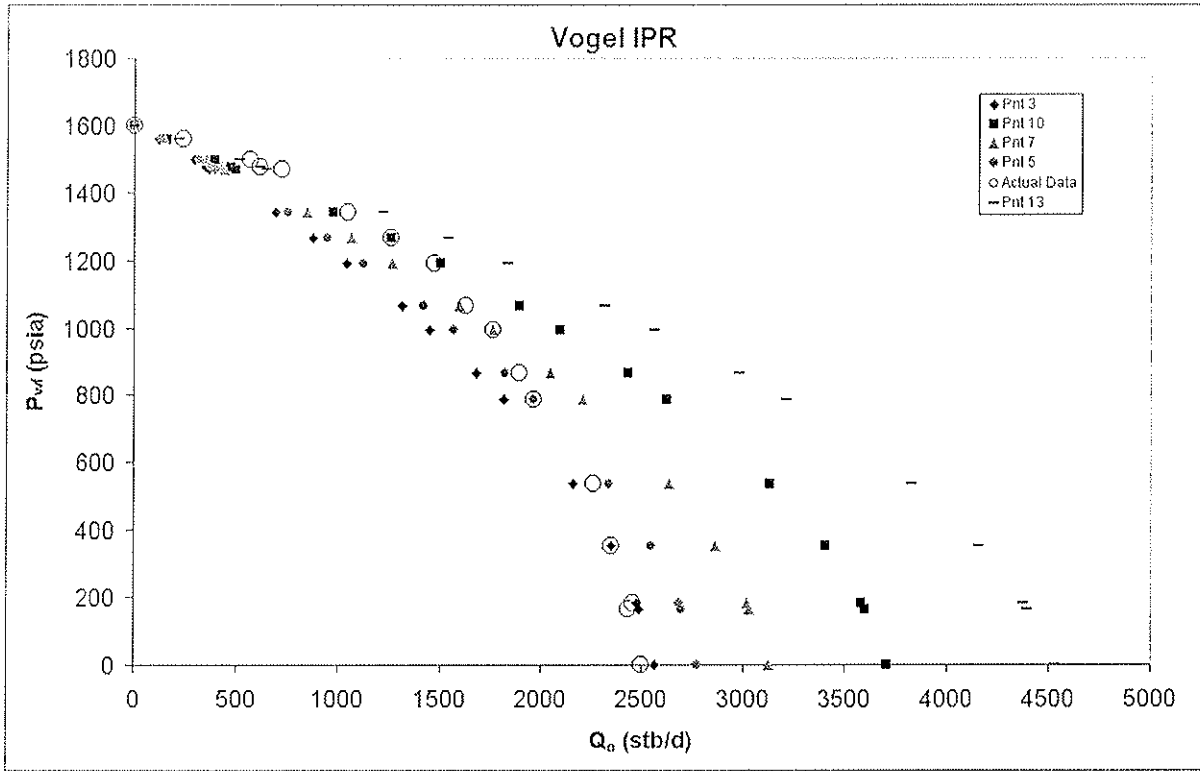
Appendix E—Current IPR Curve Comparison



Appendix F—Future IPR Curve Comparison



Appendix G—Comparison of Current Vogel IPR Curves versus Actual Production IPR Curve



Appendix H—Comparison of Current ΔP^2 IPR Curves versus Actual Production IPR Curve

